Diagnosing Discrepancies between Observations and Models of Surface Energy Fluxes in a Midlatitude Lake

ZACHARY W. TAEBEL,[a,b] DAVID E. REED,[a,c] AND ANKUR R. DESAI[a]

[a] *Department of Atmospheric and Oceanic Sciences, University of Wisconsin–Madison, Madison, Wisconsin*
[b] *Department of Marine Sciences, University of North Carolina at Chapel Hill, Chapel Hill, North Carolina*
[c] *Environmental Science, University of Science and Arts of Oklahoma, Chickasha, Oklahoma*

(Manuscript received 21 July 2021, in final form 26 February 2022)

ABSTRACT: The physical processes of heat exchange between lakes and the surrounding atmosphere are important in simulating and predicting terrestrial surface energy balance. Latent and sensible heat fluxes are the dominant physical process controlling ice growth and decay on the lake surface, as well as having influence on regional climate. While one-dimensional lake models have been used in simulating environmental changes in ice dynamics and water temperature, understanding the seasonal to daily cycles of lake surface energy balance and its relationship to lake thermal properties, atmospheric conditions, and how those are represented in models is still an open area of research. We evaluated a pair of one-dimensional lake models, Freshwater Lake (FLake) and the General Lake Model (GLM), to compare modeled latent and sensible heat fluxes against observed data collected by an eddy covariance tower during a 1-yr period in 2017, using Lake Mendota in Madison, Wisconsin, as our study site. We hypothesized transitional periods of ice cover as a leading source of model uncertainty, and we instead found that the models failed to simulate accurate values for large positive heat fluxes that occurred from late August into late December. Our results ultimately showed that one-dimensional models are effective in simulating sensible heat fluxes but are considerably less sensitive to latent heat fluxes than the observed relationships of latent heat flux to environmental drivers. These results can be used to focus future improvement of these lake models especially if they are to be used for surface boundary conditions in regional numerical weather models.

SIGNIFICANCE STATEMENT: While lakes consist of a small amount of Earth's surface, they have a large impact on local climate and weather. A large amount of energy is stored in lakes during the spring and summer, and then removed from lakes before winter. The effect is particularly noticeable in high latitudes, when the seasonal temperature difference is larger. Modeling this lake energy exchange is important for weather models and measuring this energy exchange is challenging. Here we compare modeled and observed energy exchange, and we show there are large amounts of energy exchange happening in the fall, which models struggle to capture well. During periods of partial ice coverage in early winter, lake behavior can change rapidly.

KEYWORDS: Inland seas/lakes; Heat budgets/fluxes; Surface fluxes; Lake effects

1. Introduction

Lakes are tightly coupled to Earth's climate system due to longer time scales for physical processes such as heat transfer, relative to terrestrial systems (Steele 1985). Because of this, recent impacts from climate change have been well documented in lake systems. There is an ongoing rapid and variable global warming trend within surface waters (O'Reilly et al. 2015), and this warming leads to longer duration of thermal stratification in lakes (Desai et al. 2009), decreasing ice coverage (Dugan 2021), stronger stability of stratification, and deeper daily mixing depths during peak thermal stratification (Lehman 2002). Beyond physical indicators, there are biological and chemical responses to climate change being quantified in lakes as well (Ozersky et al. 2021), and ultimately, lakes can be representative of landscape-level climate change impacts (Adrian et al. 2009). However, due to lake–climate coupling, the influence on the climate system from lakes is just as dynamic as the climatic impacts on lakes.

Besides potential global-scale feedbacks due to warming (Williamson et al. 2009), some lakes can influence regional climate as well, particularly at daily time scales, depending on lake size, depth, and regional setting. Due to their large thermal inertia, lakes act to dampen diurnal and seasonal cycles of low-level air temperature and preserve warm surface air temperatures during autumn and winter (Martynov et al. 2012; Samuelsson et al. 2010). Sensible (H) and latent (LE) heat fluxes have significant effects on regional climates; positive heat fluxes can enhance local precipitation by 20%–40%, while negative heat fluxes decrease precipitation by 70% in early summer (Samuelsson et al. 2010). The inclusion of lakes in regional climate models is also noted to alter partitioning of LE and H, increasing LE during the year and shifting the timing of maximum H fluxes from summer to autumn (MacKay 2012). Ultimately, these heat fluxes are solar radiation driven, with lakes being better at absorbing and retaining radiation than terrestrial landscapes (Xiao et al. 2020). Accurate modeling, however, depends on simulating lake surface temperature, which has been shown to be biased due to unrealistic eddy diffusion of heat transport from the deep lake to the surface (Gu et al. 2015). Recent work for mid- and high-latitude

Corresponding author: David Reed, dreed@usao.edu

DOI: 10.1175/JHM-D-21-0141.1

lakes showed winter and ice-covered periods also have a large impact on energy transfer processes, and the review of Kirillin et al. (2012) concluded that year-round observational studies are needed.

There are a number of recent lake–atmosphere eddy covariance process studies focused on the surface energy budget. Datasets from Liu et al. (2009, 2012) on a southern U.S. reservoir showed synoptic weather events have the greatest influence on monthly surface heat fluxes. Seasonal and monthly net radiation and air temperature have been shown to control surface fluxes from a Mediterranean lagoon (Bouin et al. 2012) while surface vegetation, precipitation, and net radiation control seasonal and interannual surface fluxes from a boreal mire (Peichl et al. 2013). McJannet et al. (2013) used remote sensing based scintillometry, which measures turbulent surface H fluxes, over a small irrigation dam to find that seasonal energy closure is better in winter than in summer. Vihma et al. (2009) measured surface heat fluxes over sea ice in the Weddell Sea for a limited time in the summer season and notes that differences in fluxes are due to atmospheric circulation and different ice conditions. The most comprehensive study in the literature is from Nordbo et al. (2011), which shows monthly energy budget closure varying between 57% and 112%, with annual average being 82%. While there is an emerging number of process-based lake–atmosphere observations studies (Blanken et al. 2000; Rouse et al. 2003, 2008; Shao et al. 2015), year-round datasets of lake–atmosphere heat fluxes have not been used in conjunction with lake models output to probe model uncertainty across multiple time scales.

Climate models are beginning to include lakes as part of the land surface; however, there is a lack of year-round heat flux observations needed to constrain model uncertainty. The review of Kirillin et al. (2012) notes that observational data are lacking for winter heat transport in a one-dimensional air–ice–water column while the observations of Gerbush et al. (2008) show latent heat flux to be linearly correlated with ice cover, sensible heat flux behaved in a nonlinearly with increasing lake ice coverage. While evaluation benchmarks such as ice-on and ice-free dates might match observations, with the lack of heat flux observations, evaluation of winter processes is limited and largely unconstrained within models (Leppäranta and Wang 2008) and can lead to underestimate heat fluxes and the impacts to air masses (Gerbush et al. 2008). In this study, we aim to use year-round heat flux observations from a seasonally ice-covered midlatitude lake to probe model performance using the Freshwater Lake (FLake) and the General Lake Model (GLM). Our study objectives are 1) to quantify model simulations of sensible and latent heat fluxes relative to year-round observations, 2) to test model bias in heat fluxes over changing environmental conditions, and 3) to examine lake–atmosphere heat fluxes as a function lake ice coverage.

2. Methods

a. Study lake and eddy covariance observations

Lake Mendota near Madison, Wisconsin, is one of the world's most studied lakes due to its pioneering history in foundational limnological studies, with early research in water cycling dating back to Bryson and Suomi (1952) and energy studies over 100 years ago (Birge 1915); it is currently a core study lake of the Long-Term Ecological Research program. Lake Mendota has been a focus of lake–atmosphere connections at the regional scale (Carpenter et al. 2007) and is representative of many eutrophic, medium-sized midlatitude lakes located in agricultural or urban watersheds with key physical and biogeochemical processes documented based on integration of flux and in situ observations (Baldocchi et al. 2020; Dugan 2021; Reed et al. 2018, 2019).

Lake Mendota is a 39.6-km^2 glacial dimictic lake that achieves a maximum depth of 25 m with a relatively homogeneous set of water properties as well as bathymetry (Brock 2012). The lake goes through annual cycles of freezing and melting and dates of ice-on, ice-free, and transitional periods on Lake Mendota are defined using the Wisconsin State Climatology Office long-term ice records data (http://www.aos.wisc.edu/~sco/lakes/Mendota-ice.html). On average the lake becomes ice covered around late December (median 20 December), and fully thaws in late March to early April (median 4 April), with a median duration of 104 days of ice cover, based on data from 1880 to 2020. Recent decades have shown significantly later freeze, earlier thaw, and shorter duration (Sharma et al. 2019).

Observational data from calendar year 2017 were supplied by means of an eddy covariance flux tower (registered on AmeriFlux as U.S.-PnP) on the Picnic Point (PP) peninsula on the western shore of Lake Mendota (43.089 700°, −89.415 400°). The flux tower was equipped with a sonic anemometer (CSAT3, Campbell Scientific) and inferred gas analyzer (LI-7500, LI-COR), both at a height of 12.4 m above the water surface. Temperature and relative humidity were measured at 30-min time scales using a Rotronic sensor. Eddy covariance data were processed with the TK3 software (Mauder and Foken 2015) and gap filled by means of marginal distribution sampling using REddyProc (Lasslop et al. 2010). For additional information on eddy covariance measurements including site footprint information, see Baldocchi et al. (2020).

During the ice-free periods (11 May–12 November 2017), the Lake Mendota buoy was deployed over the deepest part of the lake (43.099 500°, −89.404 500°) and is equipped with a thermistor string which gives temperature measurements from the surface to 20-m depth (Reed et al. 2018). During the winter, a temporary eddy covariance tower was collocated on ice where the buoy was deployed (Reed et al. 2019), where incoming radiation data were recorded from a net radiometer (CNR4, Kipp and Zonen). Due to the unavailability of continuous, year-round shortwave or longwave radiation measurements in situ, shortwave and longwave radiation were provided by a local NOAA SOLRAD station ~3.5 km away from the lakeshore. Comparisons of available radiation data from lake and from the SOLRAD station during the winter was significantly correlated ($p < 0.01$) at daily and hourly time scales that year-round use of SOLRAD was justified. Surface energy budget was calculated as the sum of radiation and flux terms, with outgoing shortwave radiation calculated

as a function of incoming shortwave radiation and water albedo, with albedo assumed to be constant at 0.06 during open-water periods.

b. Model descriptions

The GLM is a one-dimensional model that uses profiles of temperature, salinity, and density to calculate mixing and surface heating and cooling, including the effect of ice cover on the lake. The GLM applies a Lagrangian structure to evaluate lake characteristics across a series of vertical layers, following the methods of Imberger et al. (1978), and is not known to be sensitive to input data uncertainty (Bruce et al. 2018). Energy distribution throughout the water column is ultimately driven by the surface energy balance, where surface energy is parameterized by radiation, both longwave and shortwave, and turbulent fluxes of H and LE. As a one-dimensional model, GLM calculates H and LE through vertical gradients in temperature and vapor pressure. The sensible heat flux is calculated through the bulk aerodynamics formula:

$$\phi_H = -\rho_a c_p C_H U_x (T_s - T_a),$$

where ρ_a is air density, c_p is the specific heat capacity of air, C_H is the bulk aerodynamic coefficient for sensible heat flux, U_x is the horizontal wind speed, T_s is the water surface temperature, and T_a is the air temperature. The values of c_p (1005 J kg^{-1} °C^{-1}) and C_H (~1.3 × 10^{-3}) were assumed to be constant. The T_a and U_x were recorded at the Picnic Point flux tower, while ρ_a and T_s were calculated by the model.

Latent heat flux was calculated as

$$\phi_E = -\rho_a C_E \lambda U_x \frac{\kappa}{p} [e_s(T_s) - e_a(T_a)],$$

where C_E is the bulk aerodynamic coefficient for latent heat flux, λ is the latent heat of evaporation, κ is the ratio of molecular weight of water to molecular weight of air, p is air pressure, e_a is vapor pressure, and e_s is saturation vapor pressure of the surface layer temperature. The values of C_E (0.0013), λ (2.453 × 10^6 J kg^{-1}), and κ (0.622) were held constant. Air pressure and vapor pressures were calculated by the model, with the latter using inputs of relative humidity and air temperature to estimate e_s and e_a.

The equations for sensible and latent heat flux, in addition to shortwave and net longwave radiation, form the model surface energy balance:

$$\frac{c_p}{A_s Z_{\text{sml}}} \frac{dT_s}{dt} = \phi_{\text{SW}} - \phi_E + \phi_H + \phi_{\text{LWnet}},$$

where A_s is the lake surface area and z_{sml} is the depth of the lake surface mixed layer.

The FLake model is a one-dimensional bulk model that uses two-layer parametric representation of the lake temperature profile and calculates heat and kinetic energy for the upper mixed layer, the lower basin layer, and the bottom basin sediment, and includes lake ice and snow cover. Recent FLake results have shown more sensitivity in model output from physical lake characteristics such as depth and fetch, then model input data (Bernus et al. 2021). The FLake model computes both sensible and latent heat fluxes as a function of the lake surface temperature (Mironov et al. 2003), using Monin–Obukhov similarity relations with the surface roughness lengths calculated with respect to wind speed, potential temperature, and specific humidity. A "1/3" power law in terms of Nusselt and Rayleigh numbers is used to compute fluxes of H and LE during periods of free convection. In case of strong static stability in the surface air layer estimates of fluxes of H and LE are obtained, assuming that the transport of momentum, heat, and mass in the surface air layer is controlled by the molecular transfer mechanisms. Final heat fluxes are defined as those with greater flux magnitude between turbulent and molecular fluxes and between fluxes in forced and free convection. This calculation uses wind fetch, wind speed, air temperature, air specific humidity, surface temperature of the lake (either as water or ice/snow), and surface air pressure (Mironov and Ritter 2004; Mironov et al. 2012).

c. Snow and ice dynamics

The snow and ice dynamics in GLM assume time scales of heat conduction through ice to be small relative to time scales of meteorological forcing. When water temperature drops below 0°C a 0.05-m ice sheet is set and changes in ice thickness and snow accretion are based on a three-component ice model that includes blue ice, snow ice, and snow (Rogers et al. 1995). Upon the formation of this ice layer, the surface energy balance becomes a balance between the top layer of snow or ice and the atmosphere, where the conductive heat flux between ice and the atmosphere ϕ_o is obtained through an empirical relation for snow conductivity (Ashton 1986). LE and H are a function of the ice or snow surface. The values of the surface heat fluxes are dictated by the type of ice at the surface (blue ice, snow ice, or snow) and are modified for vapor pressure over a frozen surface (Gill 2016). When the ice sheet thickness is less than 0.05 m, the ice model is turned off and open-water conditions are restored.

Winter processes within the FLake model are more focused on ice dynamics, with snow being simplified and included in the ice surface layer. An ice-temperature-based empirical formulation of albedo and optical absorption of ice is used to vary albedo and absorption between reference values of white and blue ice as well as dry and melting snow. This process is used to account for seasonal changes of ice properties (Mironov and Ritter 2004). When ice is present, LE and H are calculated from the ice surface temperature, along with the ice thickness, ice temperature, and heat flux into the ice layer. Surface roughness and saturation water vapor pressure used in Monin–Obukhov similarity relations are calculated for ice-covered periods.

d. Model time steps and data analysis

Both the GLM and FLake model required hourly input data, which were supplied with flux tower measurements. The GLM model required an input of air temperature, shortwave and longwave radiation, relative humidity, wind speed, and

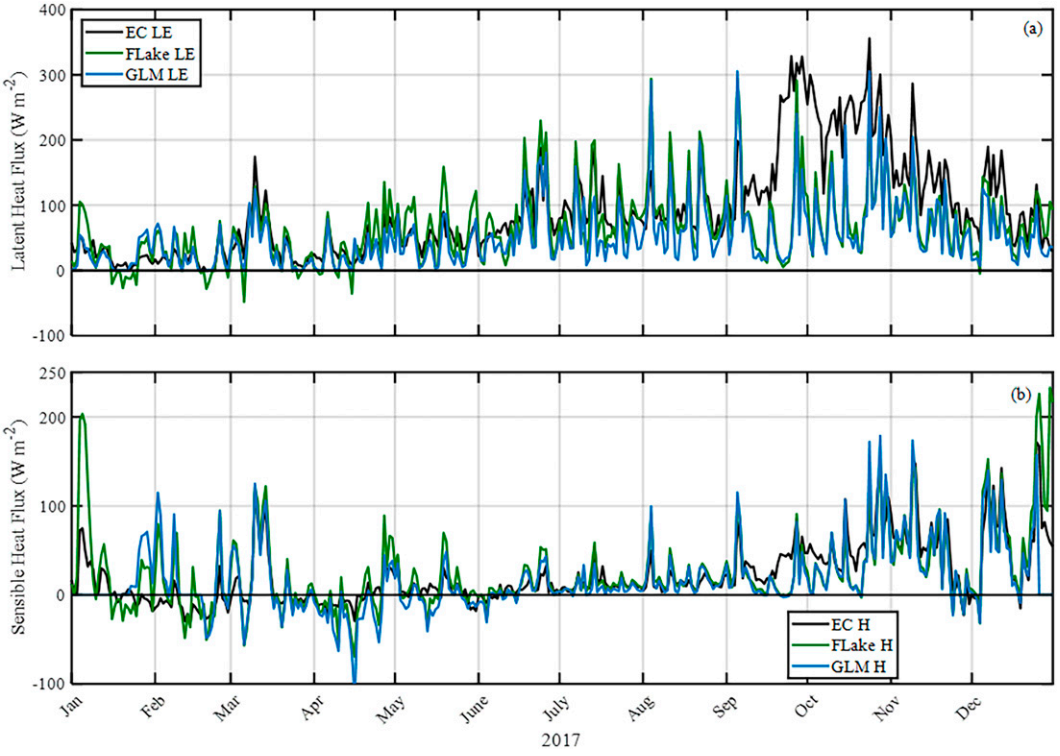

FIG. 1. Daily mean (a) latent heat and (b) sensible heat fluxes from 2017, with eddy covariance observations (black), FLake (green), and GLM (blue) modeled fluxes.

rain accumulated. Water column temperature was taken from buoy measurements. Additional input for GLM included lake wind and fetch factors, inflows and outflows, latitude and longitude, and elevation. The FLake model took a similar set of input variables including shortwave radiation, air temperature, and wind speed but also vapor pressure and cloudiness fraction, which was estimated as a ratio of the observed solar radiation to predicted solar radiation. We estimated predicted solar radiation by means of the equations for potential solar radiation given by Campbell and Norman (2012), rescaled between 1 (full cloud conditions) and 0 (clear sky).

Temporally, observed and FLake output were averaged to daily values to match GLM output time scales. Spatially, water column temperature observations and model output were averaged in between water depths. Differences in depths of water temperature output were resolved by depth averaging temperatures to match model output to observational data.

Upon averaging the data, we compared model output to observational trends through statistical values as well as sensitivity analysis. We defined outliers in the model output as points more than 1.5 standard deviations away from the first and fourth quartiles of the flux observations. For the sensitivity analysis, we averaged heat fluxes into bins based on the corresponding air temperature or humidity and noted how sensitive the heat fluxes were to changes in those atmospheric parameters. Binning was done by 5°C temperature bins and 0.1 or 0.05 kPa vapor pressure deficit (VPD) bins, with smaller VPD bins during ice transition periods due to small VPD ranges.

We compared daily averaged lake surface temperatures from the Lake Mendota buoy to model output from both the Flake and GLM models. To test how connected surface heat fluxes were to differences between observed and modeled lake surface temperature, we compared the median absolute value of the observed heat fluxes minus the modeled heat fluxes before and after 2 August, the date when the modeled surface water temperature was noted to diverge from the observations.

3. Results

a. Lake–atmosphere heat fluxes

The observed LE fluxes followed a pattern variability in the LE fluxes between January and June, with an increasing trend starting in April. An acceleration in increasing fluxes appears to occur in September after the fluxes remain quasi-steady between June and September (Fig. 1a). The LE fluxes from 15 September through 15 November accounted for 41% of the total LE from 2017. The FLake and GLM models followed a similar trend; however, the modeled LE obtained a maximum value in early summer, prior to the observed maxima. The observed LE flux period from 15 September through 15 November accounted for 23% and 27% of the total FLake and GLM LE fluxes, respectively.

When FLake LE was compared to observations (Fig. 2a), the linear fit has a slope of 0.78 ($p < 0.001$). The fitted line comparing GLM and observed LE (Fig. 2c) was closest to the one-to-one line with a slope of 0.937 ($p < 0.001$). Both

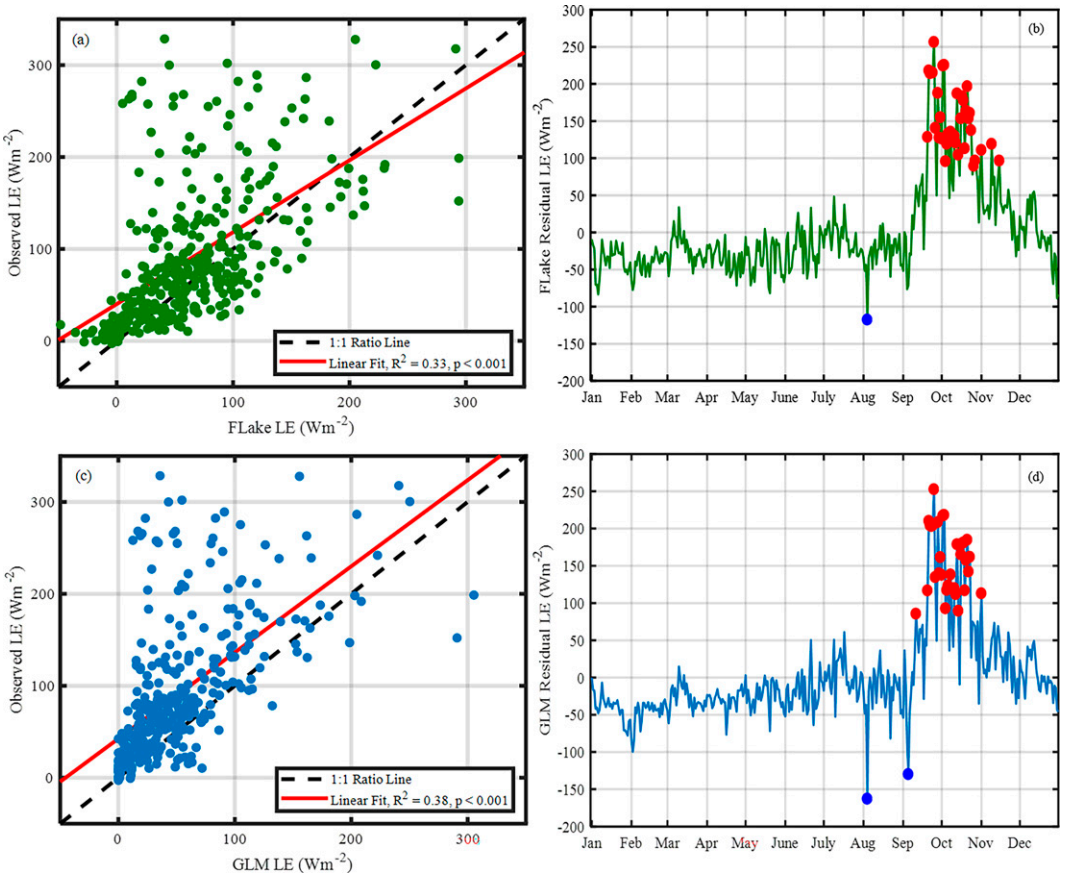

FIG. 2. Model error of (a) FLake (green) and (c) GLM (blue) latent heat (LE) daily mean fluxes. One-to-one line (black dashed), fitted line (red), and stats are included in the box. Time series residuals for (b) FLake and (d) GLM, with residuals ±1.5 standard deviations above the third and first quartile are marked (red and blue, respectively).

modeled LE fluxes had high slopes and RMSE along with low r^2 values (Table 1), relative to modeled H fluxes. In both models, the LE residuals (Figs. 2b,d) are predominantly negative from January through summer. The period of the observed LE maxima aligns with the period of the largest residuals, between 15 September and 15 November.

The observed H fluxes were predominantly smaller in magnitude than the LE fluxes; however, they followed a similar annual trend (Fig. 1b). The observed H values fluctuated between positive and negative during winter and spring before becoming positive for summer and fall. A positive autumnal maximum was observed in the H fluxes which began and ended at a similar time to the LE fluxes, with a second positive maxima observed in December. The period of the two H flux maxima from 15 September to 31 December accounted for 74% of the total H flux. The modeled heat fluxes included an autumnal maximum, and the magnitude of the modeled H fluxes was predominantly larger in magnitude than the observed during maxima. The autumnal maxima period of 15 September–15 December accounted for 60% of the FLake total H flux and 70% of the total GLM H flux.

Linear fits for the H fluxes (Figs. 3a,c) were compact about the line for the FLake model (RMSE of 21.1) and the GLM model (RMSE of 23.4); however, the slopes (FLake slope of 0.611, $p < 0.001$; GLM slope of 0.671, $p < 0.001$) and r^2 (FLake 0.63; GLM 0.55) values relative to LE fluxes were

TABLE 1. Model error values of flux heats.

	Observed vs FLake latent heat	Observed vs GLM latent heat	Observed vs FLake sensible heat	Observed vs GLm sensible Heat
Slope	0.782	0.937	0.611	0.671
R^2	0.327	0.382	0.634	0.552
RMSE	62.1	59.6	21.1	23.4
p value	4.00×10^{-33}	8.84×10^{-40}	2.45×10^{-81}	2.92×10^{-65}

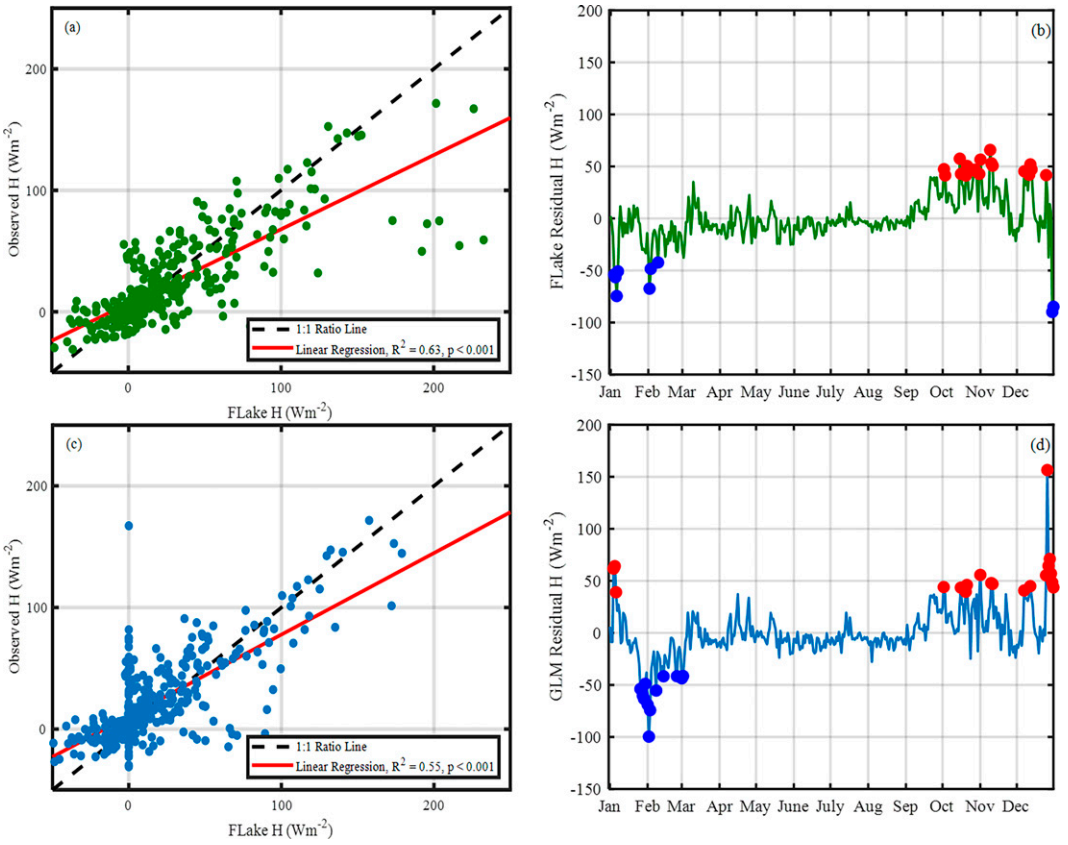

FIG. 3. Model error of (a) FLake (green) and (c) GLM (blue) sensible heat (H) daily mean fluxes. One-to-one line (black dashed), fitted line (red), and stats are included in the box. Time series residuals for (b) FLake and (d) GLM, with residuals ±1.5 standard deviations above the third and first quartile are marked (red and blue, respectively).

smaller. Unlike the LE plot, the H fluxes were generally larger for the FLake model than the observed data, particularly for the extremely large fluxes, while there was a lack of agreement in the GLM between 50 and 100 W m^{-2}, which correspond to observed fluxes of less than 50 W m^{-2}. Similar to LE, H residuals for both models (Figs. 3b,d) had high outliers observed between October and December. Both model's residual outliers were negative during the winter season, with positive outliers in the fall and into winter.

Model outliers were aligned between both models, with the majority of LE outliers co-occurring from both models and roughly half of the H outliers being co-occurring (Fig. 4). Both models had residual outliers predominantly during the period between mid-September and early November, corresponding to the period of the observed LE maxima.

b. *Lake surface temperature and energy budget*

During the buoy deployment period, the two models often overestimate the lake surface temperature relative to buoy observations (Figs. 5a,b). The GLM model surface temperature was higher than the buoy temperature for 152 of those days, with a median difference in temperature of 2.1°C. The FLake model overestimated temperatures for more days but by a lesser magnitude. For 181 days the FLake model temperature was greater than the observed temperature, with a median difference of 1.2°C. Both models overestimated the observed temperature for 151 of the 185 days. In general, the buoy temperatures at depth track modeled temperatures and the observations and model temperatures diverge at depth exactly when the surface observations and model temperatures diverge (figure not shown). At the end of the open water period, both models accumulated large energy surpluses relative to the observed buoy temperatures (Fig. 5b), with a relative gain of energy over the period.

In late summer (3 August), the observed and modeled surface temperatures diverged, consistent with the time of the largest observations to modeled heat flux disagreement. The median error in lake–atmosphere surface heat flux was more than double after the water temperature divergence (WTD) than before (Table 2). Also, the observed LE flux maxima occurred during the period following the WTD when the observed surface temperatures were quickly decreasing.

Throughout the beginning of the open water period both models tracked the observed surface energy budget well (Fig. 5c), with the FLake showing a near-zero cumulative energy budget different by the end of the summer (Fig. 5d). Starting in the early fall (8 September) both models diverged

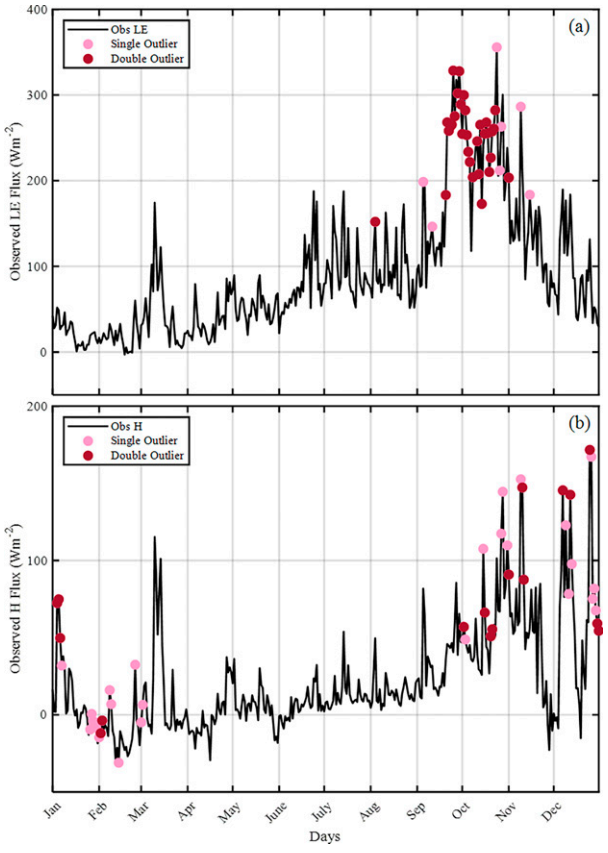

FIG. 4. Observed time series of (a) latent heat and (b) sensible heat daily mean fluxes for 2017. Days where one model had a residual outlier are noted in pink; dates where both models have residual outliers are noted in red.

from surface energy budget observations, with models overestimating the energy budget. By the end of the open water period, a large energy budget surplus was recorded by both models.

c. *Model sensitivity*

Model output of LE fluxes along with observations, were binned and regressed by temperature (Fig. 6, Table 3). During the ice-free period (Fig. 6a, 7 March–30 November) temperatures varied from −10° to 30°C. The observed LE fluxes did not have a statistically significant relationship with the air temperature ($p = 0.72$); however, the FLake model was slightly more sensitive to temperatures with a slope of −1.32 ($p = 0.01$); the GLM model fit had a slope of −1.18 ($p = 0.001$). During the transitional period (Fig. 6b, December 2017), with the air temperatures ranging from −20° to 15°C, the FLake model again had the greatest sensitivity of LE flux to changes in air temperature (slope of −4.29, $p < 0.001$) and the GLM model had a weaker sensitivity (slope of −2.39, $p = 0.03$). During the ice-on period (Fig. 6c, 1 January–6 March) the air temperature varied between −20° and 15°C. The observations (slope of −1.12, $p < 0.001$), and both FLake (slope of −3.25, $p < 0.001$) and GLM (slope of −1.62, $p < 0.001$) models were all significantly related to temperature.

LE was also regressed by VPD over the same ice-free, ice-transition, and ice-on periods. During the ice-free period (Fig. 6d), the FLake model was the most sensitive (slope of −2.16, $p = 0.01$), followed by the GLM model (slope of −1.92, $p = 0.002$), and the observed LE fluxes showed no statistically significant slope ($p = 0.96$). The transitional period (Fig. 6e) was the most sensitive for the observed data as well as both models, with the FLake flux being the most responsive to VPD changes (slope of −11.71, $p < 0.001$), followed by both the observations (slope of −6.77, $p = 0.03$) and the GLM (slope of −6.74, $p < 0.001$). During ice-on periods (Fig. 5f), the FLake fit had the greatest magnitude slope of −5.42 ($p = 0.02$), followed by GLM (slope of −4.90, $p = 0.008$) and the observed fluxes (slope of −3.48, $p = 0.02$).

The results of the bin averaged sensitivity tests for H fluxes against changing temperatures showed that H flux is more sensitive to changes in 10 m air temperature than LE fluxes (Table 3). During the ice-free period (Fig. 7a), the observed heat fluxes and the two models had similar sensitivities to temperature. The observed data had a slope of −2.03 ($p < 0.001$), the FLake model had a slope of −2.76 ($p < 0.001$), and the GLM model had a slope of −2.62 ($p = 0.01$). The H fluxes during the transitional period were the most responsive to temperature changes (Fig. 7b), with the FLake model having the highest sensitivity (slope of −9.57, $p < 0.001$), followed by observations (slope of −7.47, $p < 0.001$) and the GLM model (slope of −4.07, $p = 0.05$). During the ice-on period (Fig. 7c), the FLake model H flux was the most sensitive to changes in temperature with a slope of −6.07 ($p < 0.001$), and the GLM model (slope of −1.51, $p = 0.04$) had a similar sensitivity to the observed heat fluxes (slope of −1.13, $p < 0.001$).

The H flux was also examined over changes in VPD (Table 3). During the ice-free period (Fig. 7d) the GLM H flux and FLake H flux had nearly identical sensitivities with slopes of −2.76 ($p < 0.001$) and −2.79 ($p < 0.001$), respectively, and the observed fluxes were the least sensitive with a slope of −1.70 ($p < 0.001$). The transitional period (Fig. 7e) was again the most sensitive for all three sources of H flux, with the observed data having a slope of −21.06 ($p < 0.001$), the FLake model having a slope of −23.87 ($p < 0.001$), and the GLM model having a slope of −16.53 ($p < 0.001$). For the ice-on period (Fig. 7f) both models (FLake slope of −8.99, $p = 0.01$; GLM slope of −8.99, $p = 0.01$) were more responsive changes in VPD than observed data (slope of −5.71, $p < 0.001$).

4. Discussion

a. *Reliability of lake models*

Our first objective was to quantify differences in modeled and observed heat fluxes at daily time scales. Compared to prior work using lake models at annual time scales (Blanken et al. 2000; Rouse et al. 2003, 2008), our results suggest that there are seasonal biases which may impede model utility at

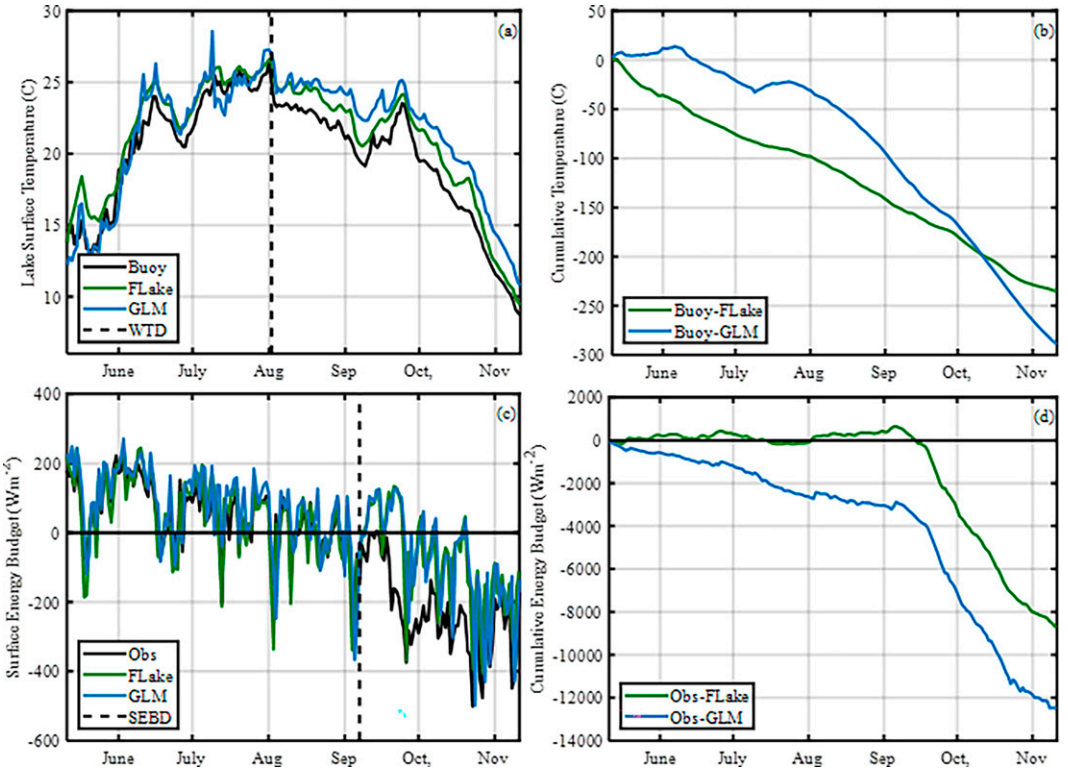

FIG. 5. (a) Water surface temperature and (c) surface energy balance from Lake Mendota buoy (black), FLake (green), and GLM (blue) modeled from May to November 2017. Black dashed line represents date of observed and modeled water temperature divergence (WTD, 3 Aug) and date of observed and modeled surface energy balance divergence (SEBD, 8 Sep). Cumulative differences from observations are shown for (b) temperature and (d) surface energy budget for the same time period.

subannual time scales (Nordbo et al. 2011). Noting Fig. 4, it can be seen that the period of greatest residual outliers coincides with the period of the observed LE flux maxima during the fall, contrary to our expectations of transition and winter period dominating discrepancies, but similar to earlier observations of large autumnal evaporation from large lakes (Bean et al. 1975; Rouse et al. 2003, 2008; Shao et al. 2015). Lake–atmosphere observation studies have identified unstable atmospheric conditions to be a cause of similar autumnal maxima in LE flux over Great Slave Lake in Canada (Rouse et al. 2003) and Lake Huron between the United States and Canada (Laird and Kristovich 2002). The impact of synoptic-scale weather also plays a critical role in surface heat exchange at variable time scales (Gerbush et al. 2008; Laird and Kristovich 2002). Neither one-dimensional lake model used in this work can reliably incorporate these kinds of boundary layer processes during their calculations, which rely exclusively on averaged surface-layer gradients (Hipsey et al. 2014; D. Mironov 2003, unpublished manuscript). Here we show a large energy storage issue late in the open water period, first in water temperature then surface energy balance.

Lake biology is a second possible factor for both the high amounts of LE fluxes and the differences in model and observed fluxes. During the lake stratification period of late May until late October, the lake experiences episodic blooms in blue-green algae, which changes carbon cycling within the lake (Reed et al. 2018), as well as lake color and albedo (Fallon and Brock 1980). Previous studies have found evidence suggesting that phytoplankton populations can influence physical lake processes by means of increased surface absorptivity driving higher surface temperatures and extra loss of energy due to heat fluxes (Jones et al. 2005; Ouyang et al. 2017;

TABLE 2. Absolute value of median differences between observed and modeled heat fluxes before and after the WTD on 3 Aug 2017.

	Median difference before WTD (W m^{-2})	Median difference after WTD (W m^{-2})
Observed latent heat vs FLake latent heat	26.84	70.15
Observed latent heat vs GLM latent heat	28.28	76.54
Observed sensible heat vs FLake sensible heat	4.86	11.32
Observed sensible heat vs GLM sensible heat	5.89	13.25

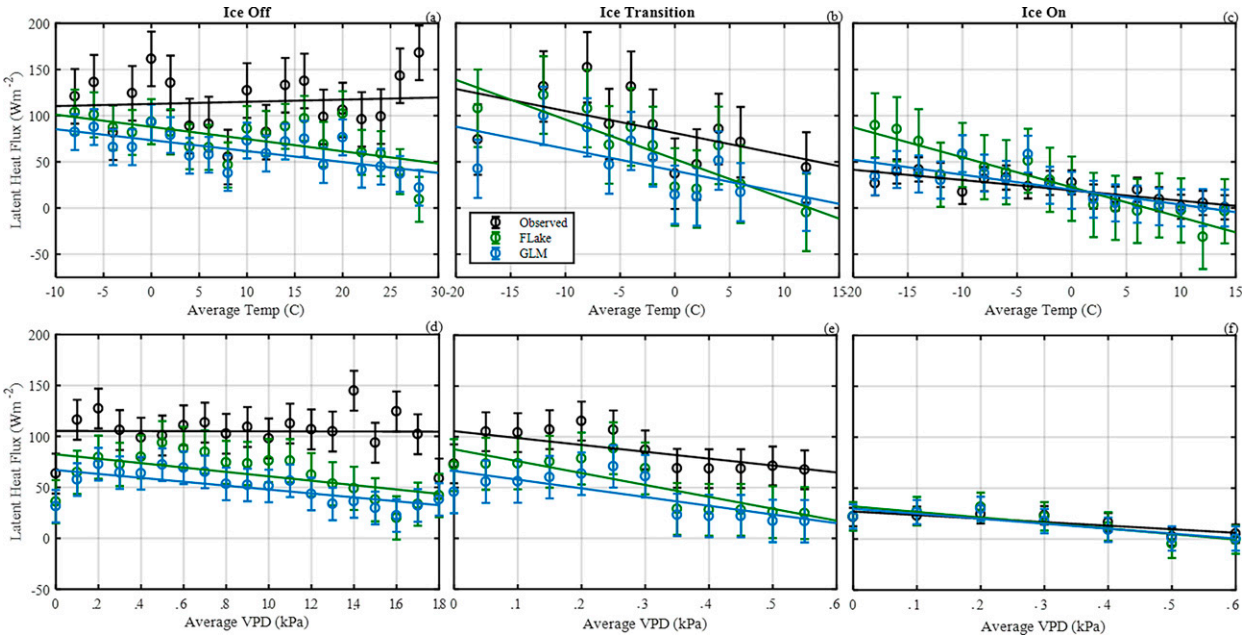

FIG. 6. Sensitives of latent heat flux to (top) air temperature and (bottom) vapor pressure deficit (VPD) changes, with observed fluxes (black), FLake (green) and GLM (green) modeled fluxes, over (a),(d) ice free periods, (b),(e) ice transitional periods, and (c),(f) ice covered periods.

Shao et al. 2015). An opportunity for future work is investigating if these correlations exist in Lake Mendota.

A third explanation may be a bias in the measurement. Kenny et al. (2017) used a large-eddy simulation (LES) of a simplified lake–land–atmosphere setting. Their study found that secondary circulations arise from differences in roughness and thermal properties at the lake–land interface. These circulations could lead to decoupling of the lake surface from the sensor depending on position and height of the system. Analysis of high-frequency time series during this period, quality control flags, flux footprints, and sensor configuration did not reveal any obvious issue. The reliability of lake–atmosphere flux measurements has been improving in literature and in postprocessing. While bias could be possible here, it should be limited in this experimental design (Vesala et al. 2012).

b. *Sensitivity of lake heat fluxes in models and observations*

Our second objective of this work was to test model bias in H and LE fluxes, and our analysis of the sensitivities suggested that the transitional periods did show a significant amount of model uncertainty in comparison to the ice-free or ice-on periods. The FLake model was the most sensitive to changes in temperature and VPD for every case studied, which may explain the large maxima in FLake heat

TABLE 3. Model error values for the temperature and VPD sensitivity test linear regressions.

	Observed	FLake	GLM	Observed	FLake	GLM	Observed	FLake	GLM
	Latent heat vs temperature ice on			Latent heat vs temperature ice off			Latent heat vs temperature transition		
Slope	−1.118	−3.250	−1.622	0.233	−1.323	−1.183	−2.386	−4.293	−2.388
p value	8.71×10^{-6}	1.35×10^{-8}	6.11×10^{-5}	0.72	0.01	1.00×10^{-3}	0.09	4.69×10^{-4}	0.03
	Sensible heat vs temperature ice on			Sensible heat vs temperature ice off			Sensible heat vs temperature transition		
Slope	1.132	−6.067	−1.512	−2.030	−2.762	−2.616	−7.472	−9.570	−4.071
p value	7.06×10^{-7}	1.16×10^{-8}	0.04	6.93×10^{-5}	2.68×10^{-7}	6.49×10^{-7}	2.07×10^{-5}	1.21×10^{-6}	0.05
	Latent heat vs VPD ice on			Latent heat vs VPD ice off			Latent heat vs VPD transition		
Slope	−0.3483	−0.5422	−0.4896	−0.0041	−0.2155	−0.1917	−0.6768	−1.1714	−0.674
p value	0.02	0.02	8.12×10^{-3}	0.96	0.01	1.53×10^{-3}	0.03	9.16×10^{-4}	5.70×10^{-5}
	Sensible heat vs VPD ice on			Sensible heat vs VPD ice off			Sensible heat vs VPD transition		
Slope	−0.5709	−0.8986	−0.7392	−0.1704	−0.2794	−0.2761	−2.1055	−2.3869	−1.6530
p value	5.01×10^{-4}	0.01	4.32×10^{-3}	1.10×10^{-4}	2.21×10^{-8}	2.54×10^{-7}	1.64×10^{-5}	1.69×10^{-5}	5.99×10^{-4}

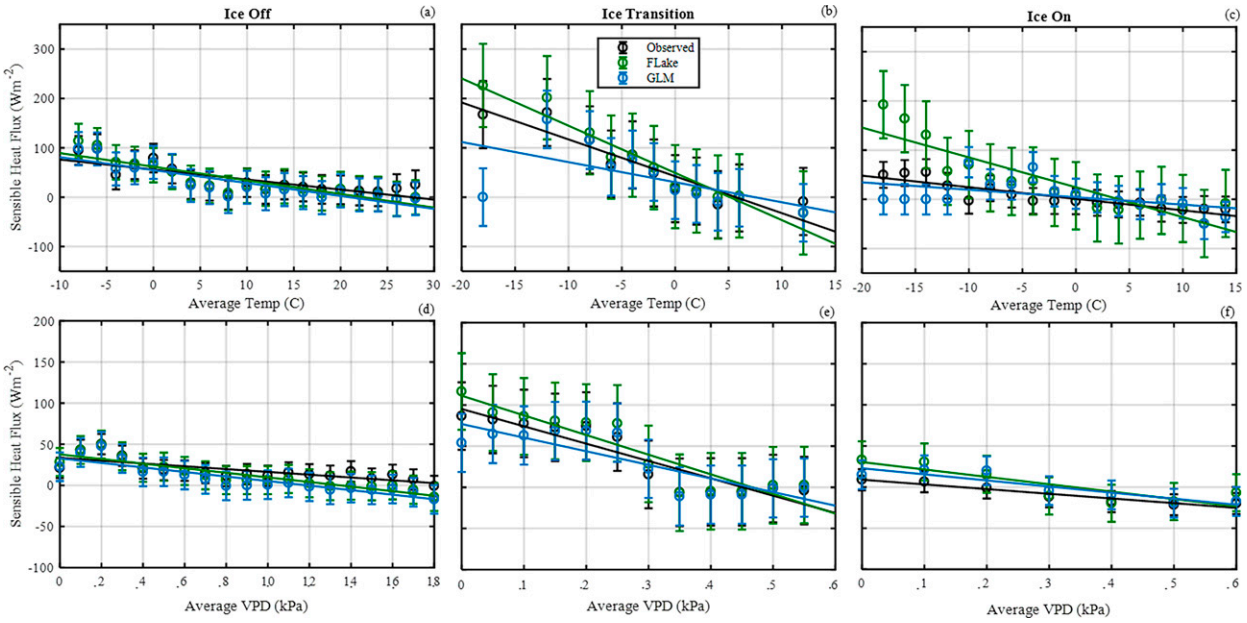

FIG. 7. Sensitives of sensible heat flux to (top) air temperature and (bottom) vapor pressure deficit (VPD) changes, with observed fluxes (black), FLake (green), and GLM (green) modeled fluxes, over (a),(d) ice-free periods, (b),(e) ice transitional periods, and (c),(f) ice-covered periods.

fluxes seen in the time series plots. The GLM model was predominantly more sensitive than the observed data but to a lesser degree than the FLake model. From the results of our experiments, we can identify a few model uncertainty trends that we observed. First, the GLM model underestimates LE fluxes throughout most of the year. Second, for both models the *H* fluxes have greater correlation to observed data than the LE fluxes. Finally, the greatest residual values occur during the period of the observed LE maxima.

Observations during ice transition period are particularly difficult. Nordbo et al. (2011) uses a year-round observational dataset to quantify lake–atmosphere heat exchange, finding month-long periods of heat being stored and emitted from a northern lake. However, additional measurements of energy in the lake–atmosphere column are needed in addition to increased temporal coverage. While technically challenging (Whitaker et al. 2016), measuring thermodynamic heat fluxes in the lake ice pack itself in greater detail would allow better connection between atmospheric heat fluxes and water column temperatures (Ozersky et al. 2021). Reed et al. (2019) was able to use a temporally limited dataset to show lake models have potentially oversimplified ice pack thermodynamics that do not include heat transfer. Advancing observations records throughout ice transitions periods is vitally important as it is clear there is thermodynamic divergence between observations and models (Ozersky et al. 2021).

c. *Sources of error in lake models and observations*

Finally, our third objective was to connect lake–atmosphere heat fluxes to the lake itself. We note a significant disagreement between observations and model output for lake surface temperature and surface energy balance. At the end of the open water period, models were 2°–3°C warmer with an accumulation of energy equal to approximately 10 days of incoming solar radiation. This noted temperature difference ultimately drives the surface energy balance difference, and prior work on the surface energy balance at Great Slave Lake found similar results to those of this study (Rouse et al. 2003, 2008). The observations of that experiment suggested that the surface radiation balance does not control the turbulent heat fluxes on a daily basis; rather, during the summer when the air is stable, the absorbed solar radiation is large and the *H* and LE fluxes are small. The opposite becomes true as the lake approaches freezing, during which the air is unstable, the absorbed solar radiation is small, and both the *H* and LE fluxes are maximized. A similar trend is shown for the evaporation rates, which are maximized just before freezing. The author suggests that the lake is capable of storing the thermal energy from summer, which creates a large gradient in energy during fall and winter and drives the strong *H* and LE fluxes (Rouse et al. 2003). Seasonally, Shao et al. (2015) found *H* to be ~25% of LE, with *H* being driven by air temperature and a weaker relationship between LE and VPD. At seasonal scales, LE increased in summer and fall, while *H* was constant throughout the year. At annual time scales, Xiao et al. (2020) found a strong correlation between LE and radiation, with LE moderated by lake cooling from outgoing longwave radiation. While at longer time scales, energy balance and heat fluxes have a relatively simple relationship, similar to Rouse et al. (2008) at daily scales, we found that multiple factors influence lake surface temperature, which makes modeling lake heat fluxes at those time scales challenging.

An analogous multimodel study focusing on lake temperature profiles shows that a comparable magnitude error in lake

water column temperatures is present for three models, including FLake (Huang et al. 2019). The authors present updated parameterization schemes within the models to correct for the differences, but they show the default settings can lead to errors in water temperature modeling. By coupling a global climate model with the FLake model, Le Moigne et al. (2016) shows lakes significantly impact the surface energy budget at the regional scale, causing changes in air temperature and pressure at varying amounts throughout the year. Errors in modeled surface water temperature would impact atmosphere heat fluxes as presented in this work, and at larger, regional scales as well.

Finally, it should be noted that the estimated measurements of surface fluxes by eddy covariance have potential biases as well, particularly during periods of low turbulence, complex turbulence, or advection. The works of Kenny et al. (2017) and Morin et al. (2018) show the strong impact of observation height and location can bias flux observations due to lake–land atmospheric circulations. As lake surface cools and then transitions to ice coverage, enhanced low-level atmospheric stability may suppress turbulence, leading to larger than typical storage or advective contribution to surface fluxes (Vesala et al. 2012). Finally, it should be noted that the eddy covariance observations made at a single height and location may not always be a representative estimate of the mean surface flux of the lake, partially due to the issues noted here. While we have processed flux data following all standard guidelines, further work on data quality filtering of lake flux observations is a critical research need as lake fluxes have particular challenges compare to other land surface flux observations.

5. Conclusions

Our investigation into model uncertainty suggested that the models have difficulty during periods of high heat fluxes. The observed maxima in LE flux were the period of greatest residual outliers, while a similar trend was noted for the *H* fluxes. These LE fluxes could drive considerable evaporation and precipitation, while the *H* fluxes could play a role in convection. Further work should be conducted to determine the impacts on boundary layer processes.

Analysis of model uncertainty in the surface energy balance is still an ongoing area of research, though improvement of heat flux calculations at small time scales can in turn improve model reliability for predicting future ice cover and carbon fluxes. This work adds to a growing body of literature that shows fall maxima in LE flux are not an aberrant event but are rather an annual occurrence. Improving how energy is modeled within lakes to account for these observed trends will yield benefits not only for surface thermodynamics, but the understanding of lakes and the success of lake models overall.

Acknowledgments. The authors thank the Atmospheric and Oceanic Science Department, Space Science and Engineering Center at UW-Madison for data collection, Hilary Dugan of the UW-Madison Center for Limnology for modeling assistance, and to Yost R at Michigan State University for editing support. Funding to support observations at the Picnic Point tower and Mendota buoy were provided by NationalScience Foundation (NSF) Atmospheric and Geospace Sciences Postdoctoral Fellowship Program (GEO-1430396) and the NSF Long-Term Ecological Research (LTER) program award to North Temperate Lakes (NTL) (DEB- 1442019JD07).

Data availability statement. Eddy covariance data from Picnic Point (U.S.-PnP) used in this study is available from the AmeriFlux data portal (https://ameriflux.lbl.gov/sites/siteinfo/US-Pnp), buoy data available from UW-Madison's LTER data portal (https://lter.limnology.wisc.edu/dataset/north-temperate-lakes-lter-high-frequency-data-meteorological-dissolved-oxygen-chlorophyll-p).

REFERENCES

Adrian, R., and Coauthors, 2009: Lakes as sentinels of climate change. *Limnol. Oceanogr.*, **54**, 2283–2297, https://doi.org/10.4319/lo.2009.54.6_part_2.2283.

Ashton, G. D., 1986: *River and Lake Ice Engineering*. Water Resources Publication, 485 pp.

Baldocchi, A. K., D. E. Reed, L. C. Loken, E. H. Stanley, H. Huerd, and A. R. Desai, 2020: Comparing spatial and temporal variation of lake-atmosphere carbon dioxide fluxes using multiple methods. *J. Geophys. Res. Biogeosci.*, **125**, e2019JG005623, https://doi.org/10.1029/2019JG005623.

Bean, B. R., C. B. Emmanuel, R. O. Gilmer, and R. E. Megavin, 1975: The spatial and temporal variations of the turbulent fluxes of heat, momentum and water vapor over lake Ontario. *J. Phys. Oceanogr.*, **5**, 532–540, https://doi.org/10.1175/1520-0485(1975)005<0532:TSATVO>2.0.CO;2.

Bernus, A., C. Ottlé, and N. Raoult, 2021: Variance based sensitivity analysis of FLake lake model for global land surface modeling. *J. Geophys. Res. Atmos.*, **126**, e2019JD031928, https://doi.org/10.1029/2019JD031928.

Birge, E. A., 1915: The heat budget of American and European lakes. *Trans. Wis. Acad. Sci. Arts Lett.*, **18**, 166–213.

Blanken, P. D., and Coauthors, 2000: Eddy covariance measurements of evaporation from Great Slave lake, Northwest Territories, Canada. *Water Resour. Res.*, **36**, 1069–1077, https://doi.org/10.1029/1999WR900338.

Bouin, M. N., G. Caniaux, O. Traulle, D. Legain, and P. Le Moigne, 2012: Long-term heat exchanges over a Mediterranean lagoon. *J. Geophys. Res.*, **117**, D23104, https://doi.org/10.1029/2012JD017857.

Brock, T. D., 2012: *A Eutrophic Lake: Lake Mendota, Wisconsin*. Ecological Studies, Vol. 55, Springer, 308 pp.

Bruce, L. C., and Coauthors, 2018: A multi-lake comparative analysis of the General Lake Model (GLM): Stress-testing across a global observatory network. *Environ. Model. Software*, **102**, 274–291, https://doi.org/10.1016/j.envsoft.2017.11.016.

Bryson, R. A., and V. Suomi, 1952: The circulation of Lake Mendota. *Trans. Amer. Geophys. Union*, **33**, 707–712, https://doi.org/10.1029/TR033i005p00707.

Campbell, G. S., and J. M. Norman, 2012: *An Introduction to Environmental Biophysics*. Springer, 286 pp.

Carpenter, S. R., and Coauthors, 2007: Understanding regional change: A comparison of two lake districts. *Bioscience*, **57**, 323–335, https://doi.org/10.1641/B570407.

Desai, A. R., J. A. Austin, V. Bennington, and G. A. McKinley, 2009: Stronger winds over a large lake in response to weakening air-to-lake temperature gradient. *Nat. Geosci.*, **2**, 855–858, https://doi.org/10.1038/ngeo693.

Dugan, H. A., 2021: A comparison of ecological memory of lake ice-off in eight north-temperate lakes. *J. Geophys. Res. Biogeosci.*, **126**, e2020JG006232, https://doi.org/10.1029/2020JG006232.

Fallon, R. D., and T. D. Brock, 1980: Planktonic blue-green algae: Production, sedimentation, and decomposition in Lake Mendota, Wisconsin. *Limnol. Oceanogr.*, **25**, 72–88, https://doi.org/10.4319/lo.1980.25.1.0072.

Gerbush, M. R., D. A. R. Kristovich, and N. F. Laird, 2008: Mesoscale boundary layer and heat flux variations over pack ice–covered Lake Erie. *J. Appl. Meteor. Climatol.*, **47**, 668–682, https://doi.org/10.1175/2007JAMC1479.1.

Gill, A. E., 2016: *Atmosphere—Ocean Dynamics*. Elsevier, 682 pp.

Gu, H., J. Jin, Y. Wu, M. B. Ek, and Z. M. Subin, 2015: Calibration and validation of lake surface temperature simulations with the coupled WRF-lake model. *Climatic Change*, **129**, 471–483, https://doi.org/10.1007/s10584-013-0978-y.

Hipsey, M., L. Bruce, and D. Hamilton, 2014: GLM-General Lake Model: Model overview and user information. AED Rep. 26, University of Western Australia, 42 pp.

Huang, A., and Coauthors, 2019: Evaluating and improving the performance of three 1-D lake models in a large deep lake of the Central Tibetan Plateau. *J. Geophys. Res. Atmos.*, **124**, 3143–3167, https://doi.org/10.1029/2018JD029610.

Imberger, J., J. Patterson, B. Hebbert, and I. Loh, 1978: Dynamics of reservoir of medium size. *J. Hydraul. Div.*, **104**, 725–743, https://doi.org/10.1061/JYCEAJ.0004997.

Jones, I., G. George, and C. Reynolds, 2005: Quantifying effects of phytoplankton on the heat budgets of two large limnetic enclosures. *Freshwater Biol.*, **50**, 1239–1247, https://doi.org/10.1111/j.1365-2427.2005.01397.x.

Kenny, W. T., G. Bohrer, T. H. Morin, C. S. Vogel, A. M. Matheny, and A. R. Desai, 2017: A numerical case study of the implications of secondary circulations to the interpretation of eddy-covariance measurements over small lakes. *Bound.-Layer Meteor.*, **165**, 311–332, https://doi.org/10.1007/s10546-017-0268-8.

Kirillin, G., and Coauthors, 2012: Physics of seasonally ice-covered lakes: A review. *Aquat. Sci.*, **74**, 659–682, https://doi.org/10.1007/s00027-012-0279-y.

Laird, N. F., and D. A. R. Kristovich, 2002: Variations of sensible and latent heat fluxes from a Great Lakes Buoy and associated synoptic weather patterns. *J. Hydrometeor.*, **3**, 3–12, https://doi.org/10.1175/1525-7541(2002)003<0003:VOSALH>2.0.CO;2.

Lasslop, G., M. Reichstein, D. Papale, A. D Richardson, A. Arneth, A. Barr, P. Stoy, and G. Wohlfahrt, 2010: Separation of net ecosystem exchange into assimilation and respiration using a light response curve approach: Critical issues and global evaluation. *Global Change Biol.*, **16**, 187–208, https://doi.org/10.1111/j.1365-2486.2009.02041.x.

Lehman, J. T., 2002: Mixing patterns and Plankton biomass of the St. Lawrence Great Lakes under climate change scenarios. *J. Great Lakes Res.*, **28**, 583–596, https://doi.org/10.1016/S0380-1330(02)70607-2.

Le Moigne, P., J. Colin, and B. Decharme, 2016: Impact of lake surface temperatures simulated by the FLake scheme in the CNRM-CM5 climate model. *Tellus*, **68A**, 31274, https://doi.org/10.3402/tellusa.v68.31274.

Leppäranta, M., and K. Wang, 2008: The ice cover on small and large lakes: Scaling analysis and mathematical modelling. *Hydrobiologia*, **599**, 183–189, https://doi.org/10.1007/s10750-007-9201-3.

Liu, H. P., Y. Zhang, S. H. Liu, H. M. Jiang, L. Sheng, and Q. L. Williams, 2009: Eddy covariance measurements of surface energy budget and evaporation in a cool season over southern open water in Mississippi. *J. Geophys. Res.*, **114**, D04110, https://doi.org/10.1029/2008JD010891.

——, Q. Y. Zhang, and G. Dowler, 2012: Environmental controls on the surface energy budget over a large Southern Inland water in the United States: An analysis of one-year eddy covariance flux data. *J. Hydrometeor.*, **13**, 1893–1910, https://doi.org/10.1175/JHM-D-12-020.1.

MacKay, M. D., 2012: A process-oriented small lake scheme for coupled climate modeling applications. *J. Hydrometeor.*, **13**, 1911–1924, https://doi.org/10.1175/JHM-D-11-0116.1.

Martynov, A., L. Sushama, R. Laprise, K. Winger, and B. Dugas, 2012: Interactive lakes in the Canadian Regional Climate Model, version 5: The role of lakes in the regional climate of North America. *Tellus*, **64A**, 16226, https://doi.org/10.3402/tellusa.v64i0.16226.

Mauder, M., and T. Foken, 2015: Documentation and Instruction Manual of the Eddy-Covariance Software Package TK3 (update). Arbeitsergebnisse 62, Universität Bayreuth, 67 pp., https://epub.uni-bayreuth.de/2130/1/ARBERG062.pdf.

McJannet, D., F. Cook, R. McGloin, H. McGowan, S. Burn, and B. Sherman, 2013: Long-term energy flux measurements over an irrigation water storage using scintillometry. *Agric. For. Meteor.*, **168**, 93–107, https://doi.org/10.1016/j.agrformet.2012.08.013.

Mironov, D., and B. Ritter, 2004: A new sea ice model for GME. Tech. Note, Deutscher Wetterdienst, 12 pp.

——, G. Kirillin, E. Heise, S. Golosov, A. Terzhevik, and I. Zverev, 2003: Parameterization of lakes in numerical models for environmental applications. *Proc. Seventh Workshop on Physical Processes in Natural Waters*, Petrozavodsk, Russia, Russian Academy of Sciences, 135–143.

——, B. Ritter, J.-P. Schulz, M. Buchhold, M. Lange, and E. MacHulskaya, 2012: Parameterisation of sea and lake ice in numerical weather prediction models of the German Weather Service. *Tellus*, **64A**, 17330, https://doi.org/10.3402/tellusa.v64i0.17330.

Morin, T., A. Rey-Sánchez, C. Vogel, A. Matheny, W. Kenny, and G. Bohrer, 2018: Carbon dioxide emissions from an oligotrophic temperate lake: An eddy covariance approach. *Ecol. Eng.*, **114**, 25–33, https://doi.org/10.1016/j.ecoleng.2017.05.005.

Nordbo, A., S. Launiainen, I. Mammarella, M. Lepparanta, J. Huotari, A. Ojala, and T. Vesala, 2011: Long-term energy flux measurements and energy balance over a small boreal lake using eddy covariance technique. *J. Geophys. Res.*, **116**, D02119, https://doi.org/10.1029/2010JD014542.

O'Reilly, C. M., and Coauthors, 2015: Rapid and highly variable warming of lake surface waters around the globe. *Geophys. Res. Lett.*, **42**, 10 773–10 781, https://doi.org/10.1002/2015GL066235.

Ouyang, Z., C. Shao, H. Chu, R. Becker, T. Bridgeman, C. A. Stepien, R. John, and J. Chen, 2017: The effect of algal blooms on carbon emissions in western Lake Erie: An

integration of remote sensing and eddy covariance measurements. *Remote Sens.*, **9**, 44, https://doi.org/10.3390/rs9010044.

Ozersky, T., and Coauthors, 2021: The changing face of winter: Lessons and questions from the Laurentian Great Lakes. *J. Geophys. Res. Biogeosci.*, **126**, e2021JG006247, https://doi.org/10.1029/2021JG006247.

Peichl, M., J. Sagerfors, A. Lindroth, I. Buffam, A. Grelle, L. Klemedtsson, H. Laudon, and M. B. Nilsson, 2013: Energy exchange and water budget partitioning in a boreal minerogenic mire. *J. Geophys. Res. Biogeosci.*, **118**, 1–13, https://doi.org/10.1029/2012JG002073.

Reed, D. E., H. A. Dugan, A. L. Flannery, and A. R. Desai, 2018: Carbon sink and source dynamics of a eutrophic deep lake using multiple flux observations over multiple years. *Limnol. Oceanogr. Lett.*, **3**, 285–292, https://doi.org/10.1002/lol2.10075.

——, A. R. Desai, E. C. Whitaker, and H. Nuckles, 2019: Evaluation of low-cost, automated lake ice thickness measurements. *J. Atmos. Oceanic Technol.*, **36**, 527–534, https://doi.org/10.1175/JTECH-D-18-0214.1.

Rogers, C. K., G. A. Lawrence, and P. F. Hamblin, 1995: Observations and numerical simulation of a shallow ice-covered midlatitude lake. *Limnol. Oceanogr.*, **40**, 374–385, https://doi.org/10.4319/lo.1995.40.2.0374.

Rouse, W. R., C. M. Oswald, J. Binyamin, P. D. Blanken, W. M. Schertzer, and C. Spence, 2003: Interannual and seasonal variability of the surface energy balance and temperature of central Great Slave Lake. *J. Hydrometeor.*, **4**, 720–730, https://doi.org/10.1175/1525-7541(2003)004<0720:IASVOT>2.0.CO;2.

——, P. D. Blanken, N. Bussières, A. E. Walker, C. J. Oswald, W. M. Schertzer, and C. Spence, 2008: An investigation of the thermal and energy balance regimes of Great Slave and Great Bear Lakes. *J. Hydrometeor.*, **9**, 1318–1333, https://doi.org/10.1175/2008JHM977.1.

Samuelsson, P., E. Kourzeneva, and D. Mironov, 2010: The impact of lakes on the European climate as simulated by a regional climate model. *Boreal Environ. Res.*, **15**, 113–129.

Shao, C., and Coauthors, 2015: Diurnal to annual changes in latent, sensible heat, and CO_2 fluxes over a Laurentian Great Lake: A case study in western Lake Erie. *J. Geophys. Res. Biogeosci.*, **120**, 1587–1604, https://doi.org/10.1002/2015JG003025.

Sharma, S., and Coauthors, 2019: Widespread loss of lake ice around the Northern Hemisphere in a warming world. *Nat. Climate Change*, **9**, 227–231, https://doi.org/10.1038/s41558-018-0393-5.

Steele, J. H., 1985: A comparison of terrestrial and marine ecological systems. *Nature*, **313**, 355–358, https://doi.org/10.1038/313355a0.

Vesala, T., W. Eugster, and A. Ojala, 2012: Eddy covariance measurements over lakes. *Eddy Covariance: A Practical Guide to Measurement and Data Analysis*, Springer, 365–376.

Vihma, T., M. M. Johansson, and J. Launiainen, 2009: Radiative and turbulent surface heat fluxes over sea ice in the western Weddell Sea in early summer. *J. Geophys. Res.*, **114**, C04019, https://doi.org/10.1029/2008JC004995.

Whitaker, E. C., D. E. Reed, and A. R. Desai, 2016: Lake ice measurements from soil water content reflectometer sensors. *Limnol. Oceanogr. Methods*, **14**, 224–230, https://doi.org/10.1002/lom3.10083.

Williamson, C. E., J. E. Saros, W. F. Vincent, and J. P. Smol, 2009: Lakes and reservoirs as sentinels, integrators, and regulators of climate change. *Limnol. Oceanogr.*, **54**, 2273–2282, https://doi.org/10.4319/lo.2009.54.6_part_2.2273.

Xiao, W., and Coauthors, 2020: Radiation controls the interannual variability of evaporation of a subtropical lake. *J. Geophys. Res. Atmos.*, **125**, e2019JD031264, https://doi.org/10.1029/2019JD031264.